JKAU: Earth Sci., **vol. 11,** pp. 143-160 (1420 A.H. / 1999 A.D.)

Lithospheric Tomography Structure Beneath Arabia using Surface Waves Group Velocities

TALAL MOKHTAR[*], CHARLES AMMON[**],
ROBERT HERRMANN[**], and HAFIDH GHALIB[***]
[*]*Dept. of Geophysics, Faculty of Earth Sciences*
King Abdulaziz University, Jeddah, Saudi Arabia.
[**]*Dept. of Earth & Atmos. Sci., Saint Louis Univ.,St. Louis, Mo, USA.*
[***]*SAIC, S. Patrick Dr., Satellite Beach, Fl, USA.*

Received: 16/6/99 Revised: 27/2/2000 Accepted: 10/4/2000

ABSTRACT. The group velocity distribution beneath the Arabian Plate is investigated using Love and Rayleigh waves. A balanced path coverage was obtained using seismograms generated by earthquakes located along the plate boundaries in the Red Sea, Gulf of Aqaba, Gulf of Aden, western Iran, Turkey, and the Dead Sea fault system. Tomographic inversions of Love- and Rayleigh-wave group velocities have been used to estimate the lateral group-velocity variations in the period range of 5 - 60 s. The Love- and Rayleigh-wave results are consistent and show that the average group velocity increases from 2.38-2.44 km/s at 5-7 s to 3.74-3.98 at 56-60 s, for Rayleigh and Love waves respectively. The tomographic results delineate first-order regional structure heterogeneity as well as a sharp transition between the two major tectonic provinces in the region, the Arabian Shield (faster than average) and the Arabian Platform (slower than average). The boundary between the fast and slow regions is sharp and coincides well with the boundaries of the Arabian Shield for shorter periods, while for longer periods, the fast regions correlate well with the boundaries of the Red Sea.

Introduction

The deployment of broadband seismic stations within the Arabian Shield (Vernon and Berger, 1997) provided an excellent opportunity to study the seismic structure of the Arabian Plate using high-quality seismic signals that were not

previously available for this part of the world. A number of recent studies have made use of the recorded broadband data (*e.g.* Sandvol *et al.* 1998, Mellors *et al.* 1997, Baker *et al.* 1997, McNamara *et al.* 1997, Rodgers *et al.* 1997, Mokhtar *et al.* 1997). In this paper we present tomographic maps showing the variations of group velocity across the Arabian Plate. In the period range between 5 and 60 s there were about 916 Rayleigh and 653 Love wave observations. Since we relied on short paths and small events, the fewest paths are those at the longest periods where we collected 376 Rayleigh wave and 178 Love-wave observations.

Tectonic Setting

The Arabian Plate consists of two major tectonic provinces, the Arabian Shield and the Arabian Platform (Fig. 1). The Arabian Shield covers about one third of the Arabian Peninsula and consists of Precambrian gneiss and metamorphosed sedimentary and volcanic rocks that have been intruded by granites (Powers *et al.* 1966, Brown, 1972). The shield consists of five micro-plates (Afif, AR-Rayn, Asir, Midyan, and Hijaz micro-plates) (Stoeser and Camp, 1985) which are separated by four ophiolite-bearing suture zones. These micro-plates are considered the remnants of Precambrian island arcs (Schmidt *et al.* 1979) that accreted to form an Arabian neo-craton around 630 Ma and which in turn were subjected to subsequent intracratonic deformation and magmatism producing the present day shield (Stoeser and Camp, 1985). Widespread Tertiary and Quaternary volcanic rocks related to initial stages of the Red Sea formation are predominant along western Arabia in the shield (Brown, 1972, Coleman, 1977).

The Arabian Platform is a large sedimentary basin that comprises about two thirds of the plate and consists of Paleozoic and Mesozoic sedimentary layers that uncomformably overlap the basement rocks and gently dip to the east (Powers *et al.* 1966). The platform sediments increase in thickness to the east and reach a thickness of 10 km or more beneath the Mesopotamian foredeep (Brown, 1972). The western platform sediments are relatively undeformed but deformation increases to the east towards the foredeep and the Zagros and Taurus mountains.

Five tectonic boundaries surround the Arabian Plate (Maamoun, 1976): The continental collision boundary between the Arabian Plate and the Persian and Turkish Plates along the Zagros and Taurus mountains in the north and northeast; the subduction boundary in the Gulf of Oman region in southern Iran (Makran subduction zone); the transform fault boundary along the Owen Fracture zone in the southeast; the transform fault boundary along the Dead Sea fault system in the northwest; and the spreading axis along the Red Sea and Gulf of Aden in the west and southwest. All of these boundaries are tectonically

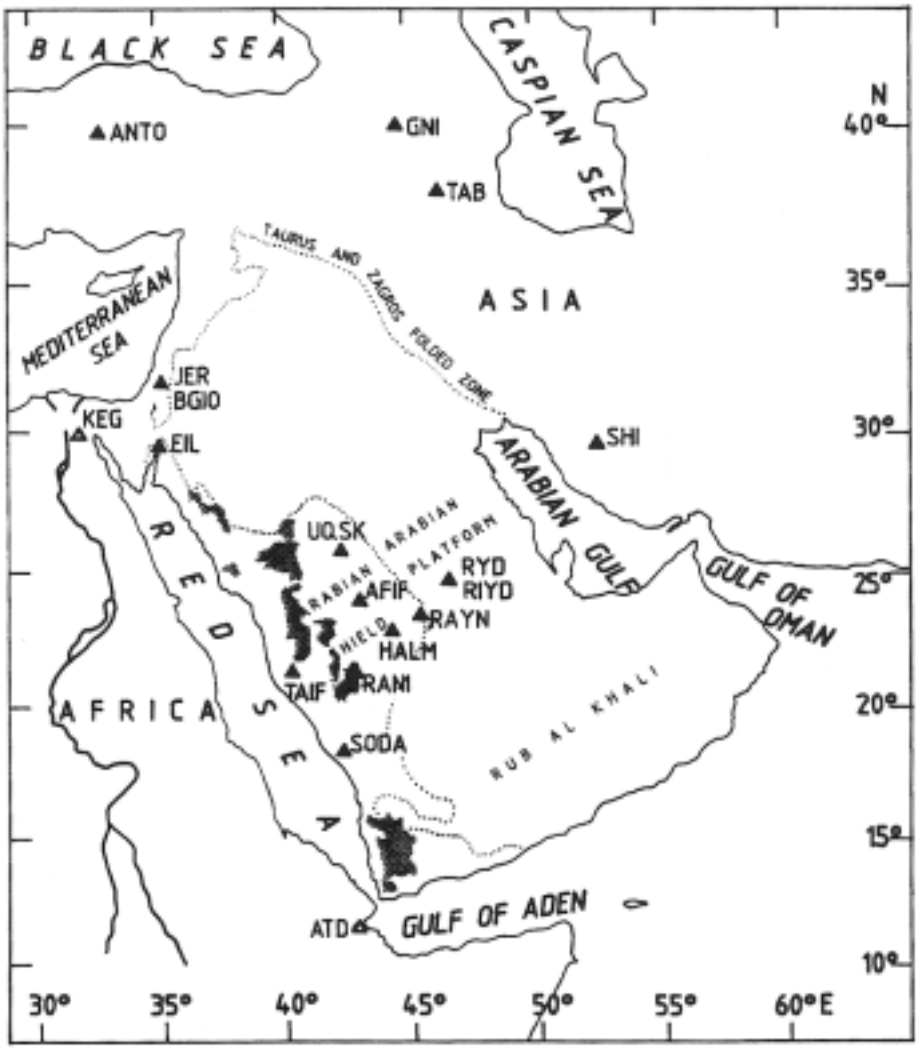

FIG. 1. Tectonic provinces of the Arabian Plate and the different plate boundaries. Seismic stations used in this study are shown.

active and produce an appreciable number of earthquakes, especially along the boundary associated with the Zagros mountain belt in the northeast.

Previous Geophysical Investigations

The shear-wave velocity structure of the two major tectonic provinces was modeled by Mokhtar & Al-Saeed (1994) using surface wave dispersion inversion. The model of the Arabian Platform was found to be similar to that of East Africa. It consists basically of an upper crust, 20 km thick, with shear wave velocity of 3.4 km/s, overlying a 20 km thick lower crust with shear wave velocity of 4.0 km/s. Mokhtar (1995) used waveform modeling to verify the Arabian Platform shear-wave velocity models of Mokhtar and Al-Saeed (1994). The Arabian Shield velocity model consists of an upper and lower crust of comparable thickness to those of the platform with P-wave velocities of 6.3 km/s and 7.0 km/s for the upper and lower crust respectively (Mooney *et al.* 1985). S-wave velocity is 3.6 km/s and 3.88 km/s for the upper and lower crust (Mokhtar and Al-Saeed, 1994). The depth to the mantle is about 45 km beneath the platform and it decreases to the southwest and reaches about 38-40 km in the southwestern part of the shield (Mokhtar and Al-Saeed, 1994, Mooney *et al.* 1985, Badri, 1991). Sandvol *et al.* (1998) estimated the lithospheric mantle and crustal velocity structures beneath the Arabian Shield through the modeling of teleseismic P waves recorded by the temporary broadband array used in this study. Application of the receiver function techniques showed that the crustal thickness of the shield area varies from 35 to 40 km in the west adjacent to the Red Sea, to 45 km in central Arabia. These results are consistent with the previous results from surface-wave inversion (Mokhtar and Al-Saeed, 1994), and the deep seismic refraction results (Mooney *et al.* 1985, Badri, 1991). Ghalib (1992) utilized Rayleigh-wave fundamental-mode group-velocity observations from five analog seismic stations to investigate the three-dimensional seismic structure of the Arabian Plate. He reported the presence of two discontinuities at 15-22 and 35-55 km depth and the crustal velocity was found to be higher under the Arabian Shield than under the rest of the plate.

Mokhtar and Al-Saeed (1994) presented two sets of dispersion data (Path II and Path III in their work) for Love and Rayleigh-waves for the Arabian Platform and one set for Rayleigh-wave for the Arabian Shield (Path I). Path II extends from the eastern part of the Gulf of Aden to RYD station, while Path III connects the events in southern Iran to RYD station. There were no reliable Love-wave dispersion data for the Arabian Shield reported by Mokhtar and Al-Saeed (1994). Figure 2 shows the resulting average group velocity of Rayleigh-waves compared to the values of Path I-Path III obtained by Mokhtar and Al-Saeed, 1994). The Arabian Shield has a higher group velocity than the average

while the Arabian Plate group velocity values are lower than the average. Similar behavior is observed for Love-wave as shown in Fig. 3.

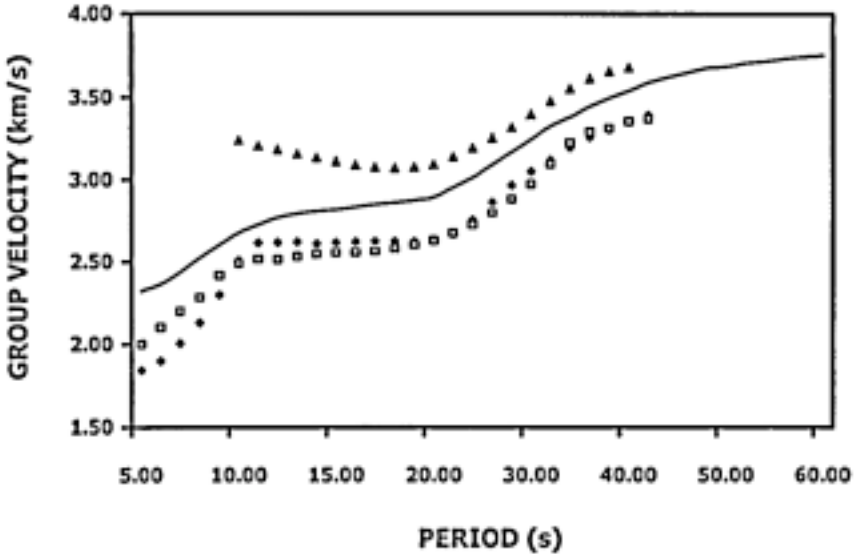

FIG. 2. Average group velocities for Rayleigh-waves (solid line) compared to those of the Arabian Shield (solid triangles) and the Arabian Platform (Solid diamonds for Path II, and open squares are for Path III) as obtained by Mokhtar and Al-Saeed (1994).

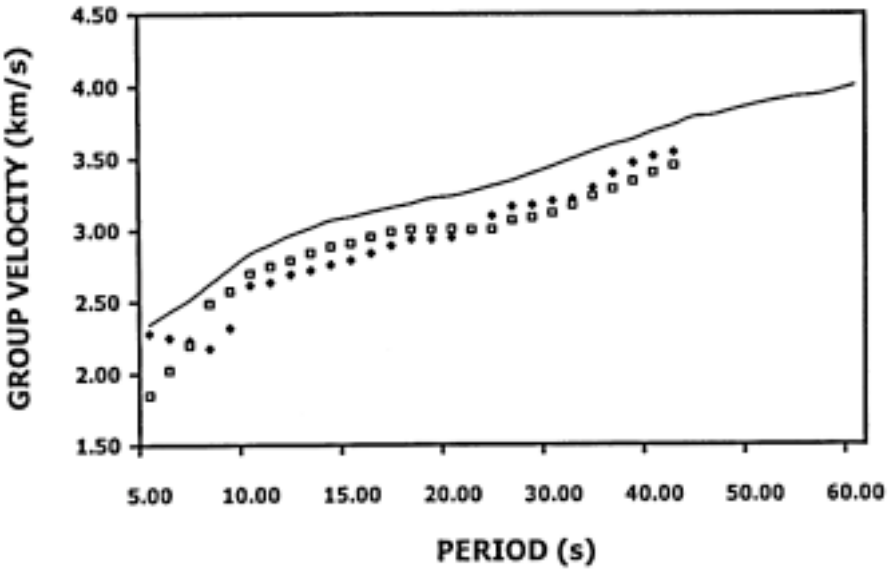

FIG. 3. Average group velocities for Love-waves (solid line) compared to those of the Arabian Platform (See Fig. 4 for explanation).

Wu and Levshin (1994), used surface wave tomography to provide group velocity maps of East Asia. Also, Ritzwoller and Levshin (1998) and Ritzwoller *et al.* (1998) produced tomographic maps from surface wave group velocities across all of Eurasia, Central Asia, Western China, and parts of the Middle East. These maps were at a length scale intermediate between regional and global surface waves studies and extends for periods in the range 20-200 s. Group velocity maps from these studies for 20-30 s period display low velocity anomalies associated with most of the known sedimentary basins across Eurasia especially those with Love waves. On the other hand, 20 s Rayleigh and Love waves group velocity maps from these studies correlate well with the high velocity regions associated with the massive basaltic flows in northern Ethiopia near the southwestern boundary of the Arabian Plate.

Observations

In the present paper, surface-wave group velocities generated by earthquakes located along the boundaries of the Arabian Plate in the Red Sea, Gulf of Aqaba, Gulf of Aden, western Iran, Turkey, and the Dead Sea fault system were used. The observations were compiled from four different sources: 1) Digital broadband seismograms from the Saudi Arabian 1995/1996 temporary seismic network deployment which include about 494 seismograms from earthquakes that occurred during the period December 31, 1995 to September 15, 1996. This data represents about 50% of the Rayleigh-wave and about 60% of the Love-wave data; 2) Digital seismograms recorded by the permanent broadband stations in the region for the period between1990 and 1996 which represent 26% of the Rayleigh-wave and 36% of the Love-wave data; 3) Analog observations of Rayleigh waves from the regional WWSSN stations recorded between 1970 and 1979 which represent 19% of the total Rayleigh-wave data; and 4) Analog observations from RYD station recorded between 1981 and 1987 and represent 5% of both Rayleigh- and Love-wave data.

Figs. 4 and 5 show the great circle path coverage along which dispersion measurements were made for both Love- and Rayleigh-waves. A total of 987 Rayleigh-wave and 682 Love-wave paths were available. A maximum of 916 rays for Rayleigh and 682 rays for Love were used in the period range of 11-13 seconds (this is the average of the total number of ray paths over the 3 periods). The number of great circle paths decreases for longer periods and reaches 376 for Rayleigh and 178 for Love at 56-60 s periods. The seismic stations used in this study are also shown in these figures. They include the XI95-96 IRIS digital broadband stations of AFIF, HALM, RAYN, RIYD, RANI, TAIF, UQSK, and SODA; the regional broadband GSN seismic stations of ANTO, GNI, BGIO, KEG; a Geoscope station ATD; and the WWSSN stations from which analog data were digitized (TAB, SHI, EIL, JER, and RYD).

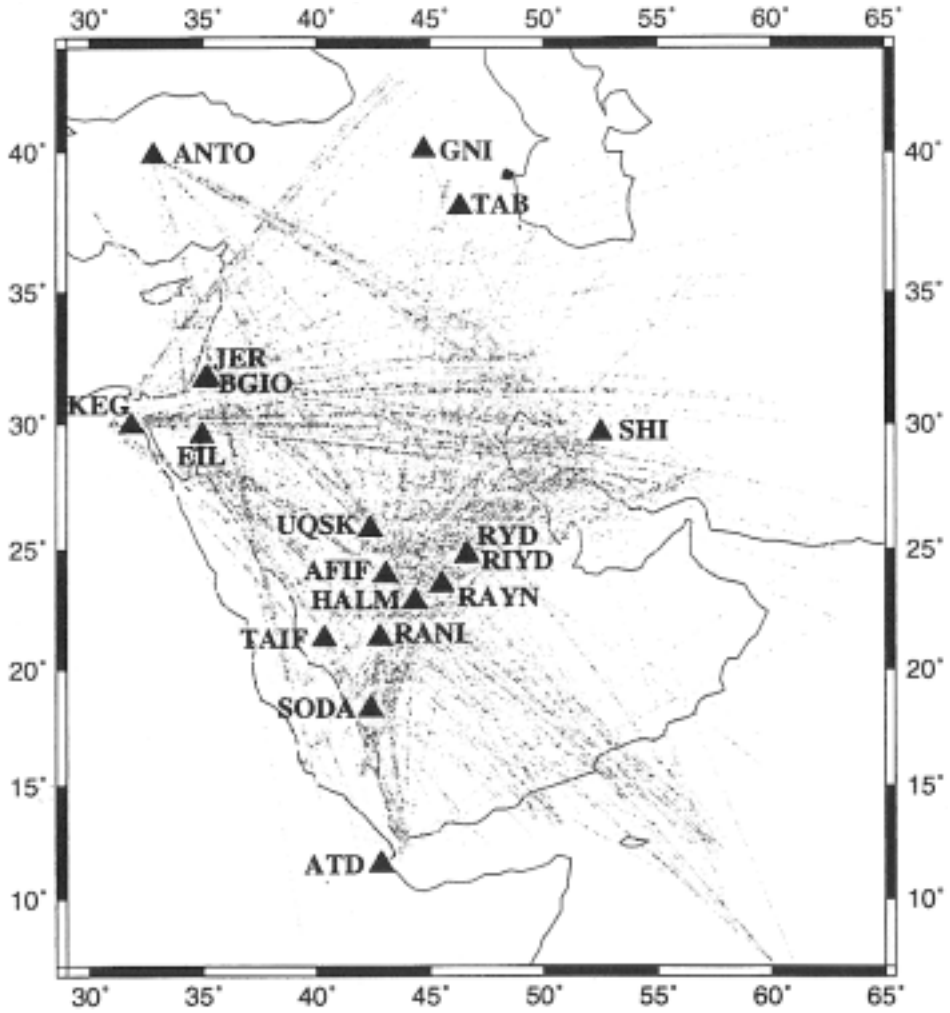

FIG. 4. Distribution of ray path coverage for Love-wave.

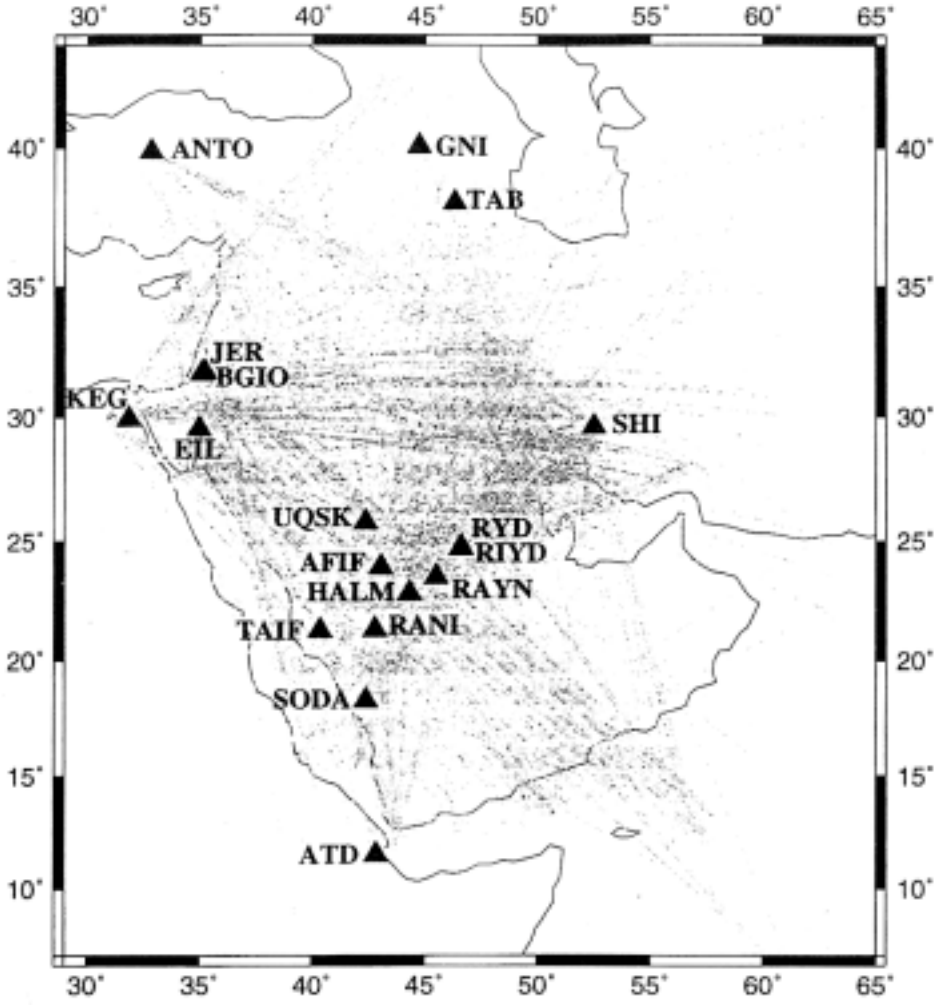

FIG. 5. Distribution of ray path coverage for Raleigh waves.

The regional scale tomographic maps presented below provide significant constraints on the shear velocity and crustal thickness of the Arabian Plate. Mainly the seismic stations inside the plate or very close to its tectonic boundaries recorded these data avoiding long paths that may traverses a number of tectonic provinces and geological features. Maps showing the distribution of surface waves group velocities propagating at regional distances in the period range of interest in this study are very useful in constraining the regional structure of the crust and upper mantle. The stations deployed in Saudi Arabia provided significant coverage of the Arabian Shield. There is also significant coverage of the western part of Iran and all of Iraq.

Methods of Analysis

Seismic wave tomography method is a similar technique to the whole body scanning method that medical physicists use. First the phase and or group velocities of surface waves are measured for hundreds of earthquakes and recording stations. A best fitting model of velocity structure is then constructed, the computed group velocities of this model are compared to the observed values along each path, and the model is adjusted by the back projection iterative procedure. The detailed analysis of seismic tomography can be found in Woodhouse and Dziewonski (1984), Nolet (1987), and Iyer and Hirahara (1993). Following Levshin *et al.* (1989), the method can be summarized as follows;

The group velocity map $U(\theta, \phi)$ at each period and the wave type can be estimated by attempting to minimize the following function:

$$\sum_{i=1}^{N} [w_i (t_i^{obs} - t_i^{pred})]^2 + \lambda \int_S |\nabla U(\theta, \phi)|^2 \, dA,$$

where

$$t_i^{pred} = \int_{P_i} U^{-1} (\theta, \phi) \, ds.$$

Here, p_i represents the *i*-th wave path, w_i is the weight associated with *i*-th path, $w_i = \sqrt{m}(g_i/\sigma_i)$, where m is the number of raw measurements that compose the cluster that produced this measurement *i,* and g_i is a weight which depends on the quality of the measurement. t_i^{obs} and t_i^{pred} are the observed and the predicted group travel times along the *i*-th path and *S* is the region on which the tomographic inversion is performed. Choosing different values of the trade-off parameter, λ changes the trade-off between the fit to the data and the 'smoothness' of the resulting group velocity map. 'Smooth' here is defined in terms of the spatial gradient of the model.

The results of regional tomographic inversion of dispersion data from Rayleigh and Love waves across Arabia were obtained using single station measurements of group velocity and applying the multiple filtering analysis tech-

nique (Dziewonski *et al.* 1972, Herrmann, 1987). The dispersion measurements were obtained at each period in the range 5-20 s and at even periods only in the range 22-60 seconds. Observations from each period are inverted separately and the images from adjacent periods were averaged. We parameterized the regional slowness variations using a uniform, $1^\circ \times 1^\circ$ grid of constant-slowness cells. Group velocity maps were produced using a conjugate-gradient least square algorithm (Paige and Sanders, 1982). Laplacian smoothness constraints were incorporated in the inversion and thus we minimized a combination of group travel time misfit and a Laplacian measure of a two dimensional model roughness. The balance between group delay misfit and minimal roughness is selected empirically by running inversions with a range of smoothness importance weights and selecting the value that produces the simplest model and still satisfactorily matches the observed group delays. The resulting velocity variations are presented as percent velocity perturbations from the average velocity of all the measurements (which was the initial model).

It is assumed that the measured waves have propagated along the great circle path connecting the source and the receiver. Ritzwoller and Levshin (1998) discussed the problems expected to result from several factors such as off-great circle propagation, azimuthal anisotropy, and systematic event mislocations near subducting slabs, and argued that these effects should not alter the tomographic maps of group velocities strongly beyond the resolution estimates. In addition, our use of short-distance paths helps minimize the likely deflection of the path from the great-circle arc.

Resolution

Estimating the resolution in a tomographic inversion is not a trivial task because resolution depends on complex factors such as the number of crossing rays, the density of sources and receivers, as well as the random and possible systematic uncertainty in the measurements. To estimate our resolving capability, we used standard "checker-board" tests. Specifically, we tested two models, each of the two models consists of $1^\circ \times 1^\circ$ cells in which a velocity perturbation of $\pm$ 10% of the average were chosen to have a dimension of $3^\circ \times 3^\circ$ for the first model (Fig. 6) and $8^\circ \times 8^\circ$ for the second model (Fig.7). The checker board test results show that features of dimension $8^\circ \times 8^\circ$ are reasonably recovered especially in the short period ranges where the number of ray paths is maximum. In contrast, features of dimensions smaller than that are hardly recognized using the current coverage of the data available. The precise amplitude of the anomaly is difficult to estimate due to dependence on damping and smoothing (which complicates tests involving models with sharp contrasts) but the pattern of variations is reasonably well reconstructed. We performed tests

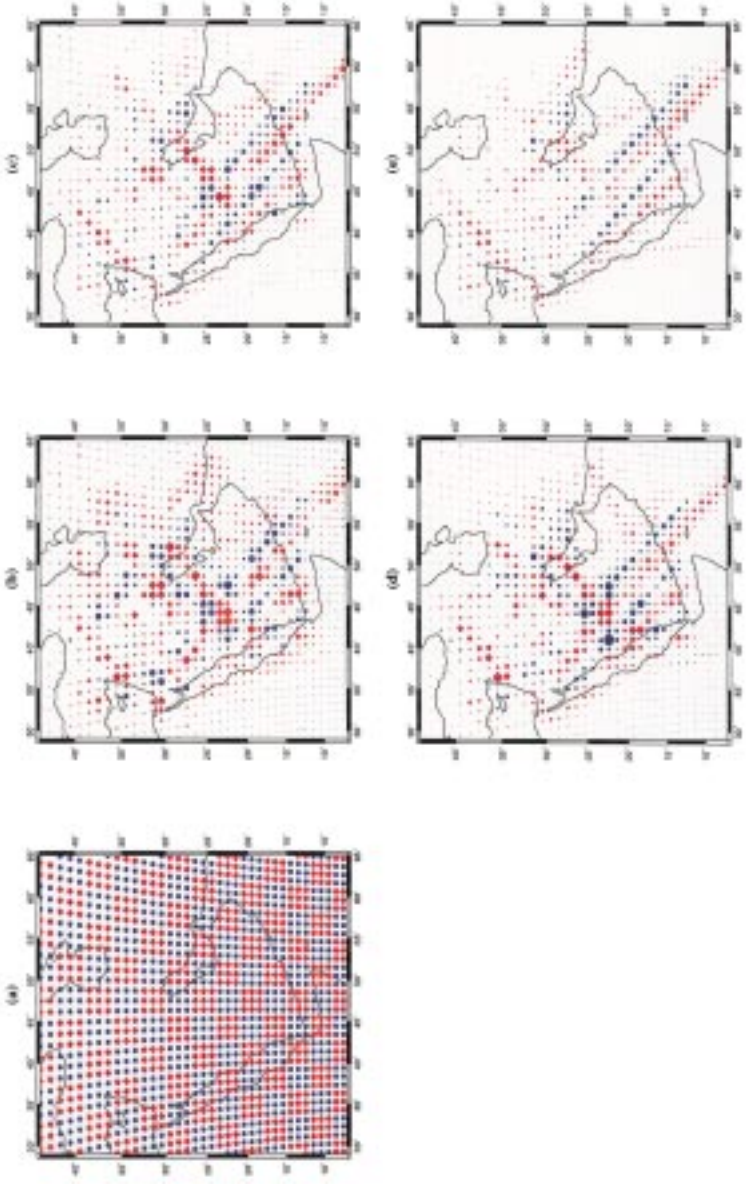

FIG. 6. Checkerboard test results:
a) The original velocity perturbation model using a feature of $3^{o} \times 3^{o}$ in dimension.
b) Tomographic inversion results for Rayleigh-waves using the maximum number of rays.
c) Rayleigh-waves results using the minimum number of rays.
d) Love-waves results using the maximum number of rays.
e) Love-waves results using the minimum number of rays.

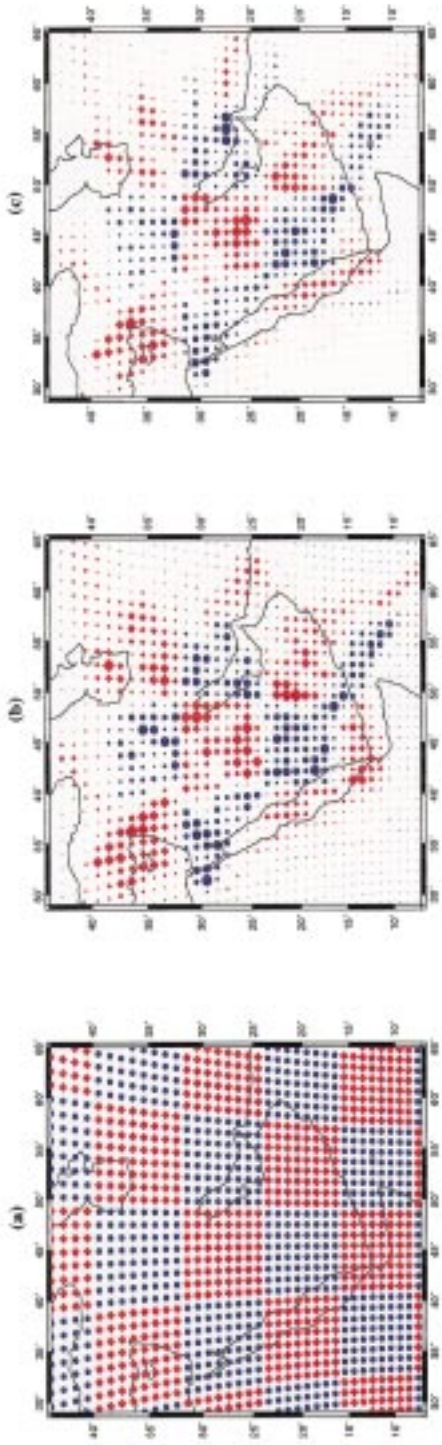

FIG. 7. Checkerboard test results using a $8^{o} \times 8^{o}$ velocity perturbation model. a, b, c, d, e are as in Fig. 6.

for both Love and Rayleigh waves and tested the resolution for the maximum and minimum number of ray paths in each case.

Rayleigh- and Love-wave Group-velocity Variations in the Middle East

In Figs. 8 and 9, the tomographic images constructed for Love and Rayleigh waves are shown respectively. Each map shows the average group velocity variations for three adjacent periods and at the top of each map, the average group velocity for that period range and the average number of rays for the same periods are listed. One striking observation in these maps is the consistency of the results from both Rayleigh and Love waves. The distribution of faster and slower group velocities, than average regions, is strikingly similar in both data sets especially in the short periods. It is clearly evident that the Arabian Shield is characterized by relatively higher than average seismic velocity, while the rest of the Arabian Platform covered by an eastward-thickening sedimentary section has in general slower than average velocity. The boundary between the fast and slow regions is sharp and correlates well with the boundaries of the Arabian Shield especially at periods shorter than 10 s. For longer periods, a fast region correlates well with the boundaries of the Red Sea especially for the Rayleigh waves. However, in general, the seismic velocity is higher in western Arabia than in the eastern or the north eastern parts of the plate. The resolution diminishes for long periods where the number of rays becomes smaller. The average group velocity of Love waves increases from about 2.44 km/s at 5-7 s to 3.98 km/s at 56-60 s, while that of Rayleigh waves increases from 2.38 km/s at 5-7 s to 3.74 km/s at 56-60 s. The mean velocities at the longer periods (50-60 s) are about 8% slow for Love waves, but only about 3% slow for Rayleigh waves.

We do not have adequate coverage to image the southeastern part of the Arabian Plate where it is covered mainly by the Empty Quarter region. Also, the localized fast anomaly located east of the Gulf of Aden and the slow feature located in eastern Mediterranean region should be interpreted as a result of bias in the data since there is not enough traverses crossing these two regions. In general, the resolution of the oceanic structure south of the Arabian Plate is limited to a small region that produces an apparent localized heterogeneity.

The obtained results are consistent with those of Ghalib (1992) who analyzed the analog seismograms recorded at stations TAB, SHI, EIL, and JER to outline the lateral variation of shear-wave velocity beneath the Arabian Plate at depths from 5 to 80 km. He concluded that the shear wave velocity within the crust is higher in the shield region than in the platform area for depths less than 40 km, but the pattern is reversed at depths below 40 km. This is consistent with the conclusion of Woodhouse and Dziewonski (1984) regarding the possible existence of low-velocity anomalies along the western and southwestern Arabian Plate.

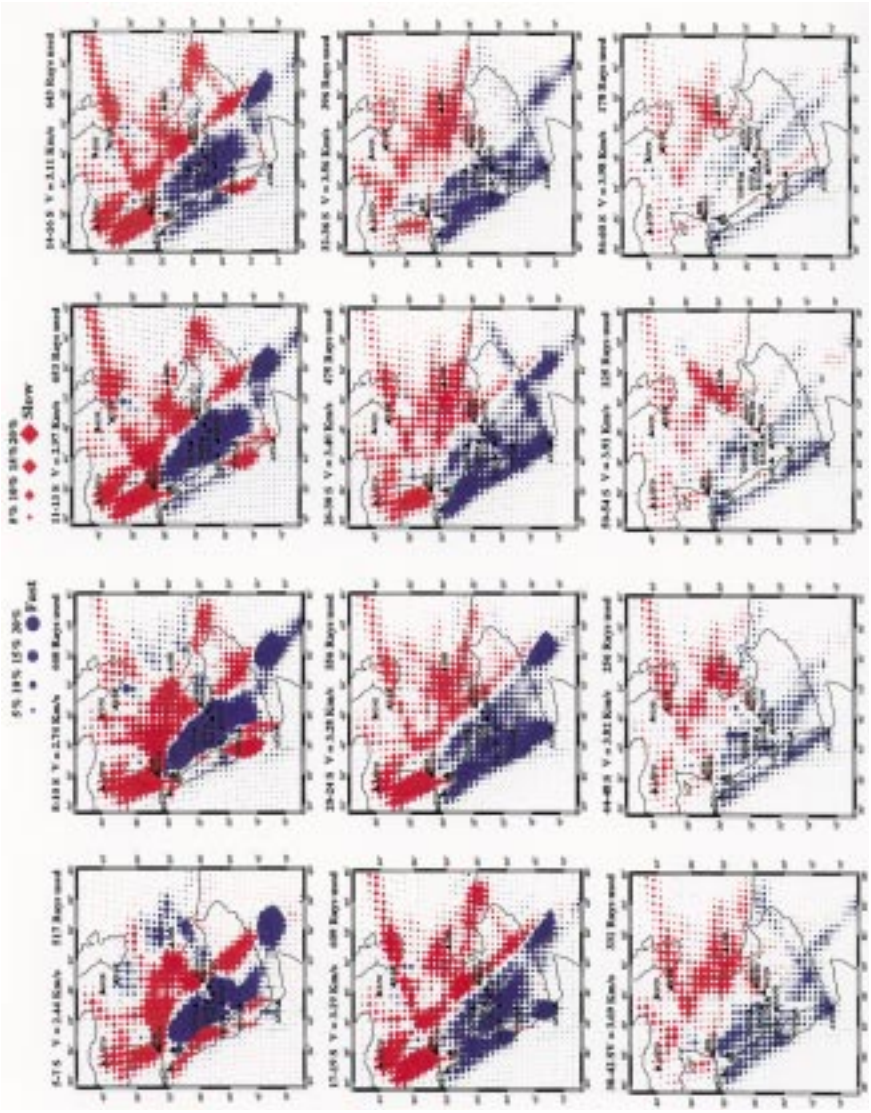

FIG. 8. Tomography map of the Arabian Plate Love-wave group velocity. The legend shows the percentage of the velocity perturbations. The average group velocity and the number of rays used are given for each period group.

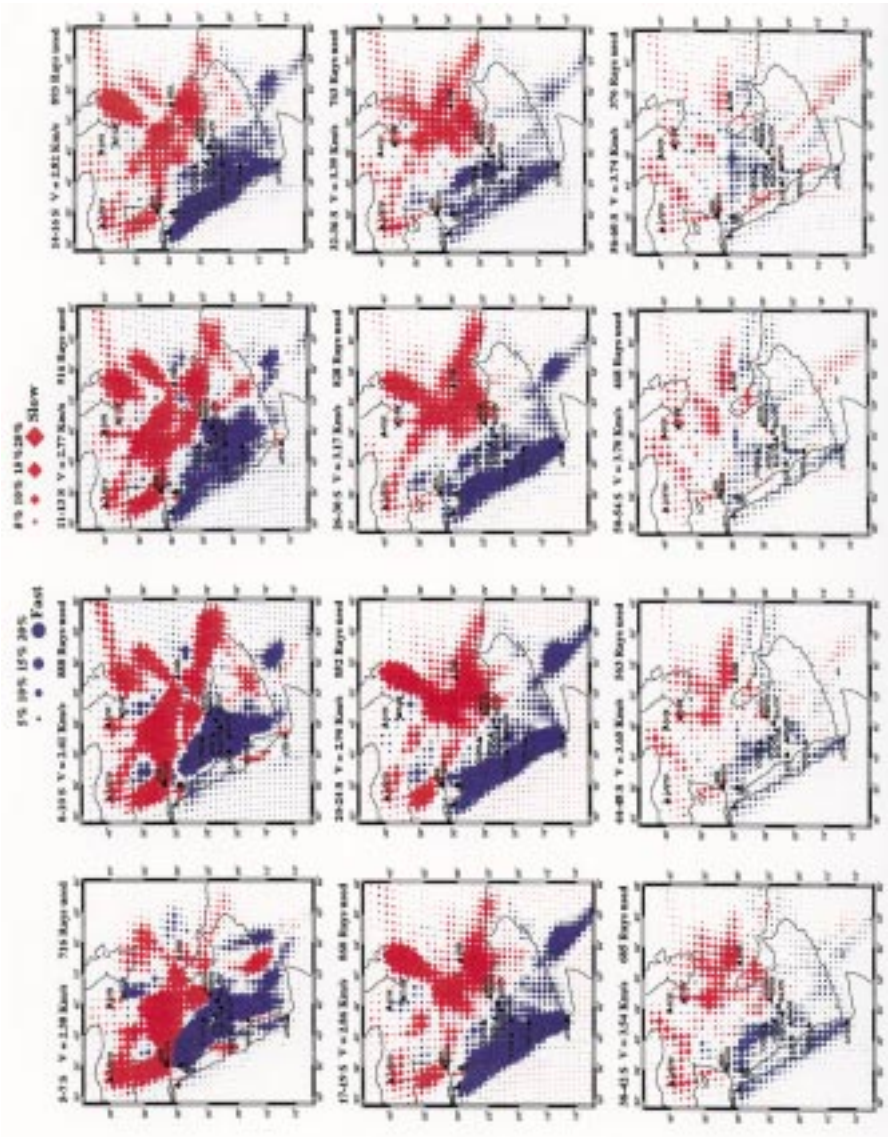

FIG. 9. Tomography map of the Arabian Plate Rayleigh-wave group velocity.

Roobol and Al-Rehaili (1997) suggested that the presence of a more or less linear distribution of volcanic fields in western Arabia is evidence for a new rift system in the region that has been developing for the past 12 million years. This system is independent from the widely accepted main rift model of the Red Sea and Gulf of Aden. Robol and Al-Rehaili (1997) argued that along this trend of volcanic features, fractures are opening and closing and that seismic and micro-seismic activities are produced that coincide with this fracture system, and that this new rift system is related to deep seated north-northwest trending faults parallel to the Red Sea. They did not present any locations for earthquakes that show the presence of recent seismicity that correlates with the suggested new rift system. In spite of this, and even if there were some-kind of seismic activities associated with these fractures and volcanic fields, the present study does not support the argument that these surficial features has any relationship to a deep seated features. One would expect that the seismic velocity distribution would reflect the heterogeneity of the material beneath such rift. High density and high seismic velocity from the upper mantle material would reveal itself in a somewhat linear trend parallel and in line with the suggested new linear rifting system and well distinguished from the surrounding crust that is being rifted. We do not see evidence for strong heterogeneity within the Arabian Shield.

References

Badri, M. (1991) Crustal structure of central Saudi Arabia determined from seismic refraction profiling. *Tectonophysics,* **185:** 357-374.

Baker, G. E., Barker, T. G. and **McLaughlin, K. L.** (1997) Sources and propagation effects on regional phase amplitudes in the Middle East (Abstract). *American Geophysical Union Fall Meeting* **78**(46): 46, F428.

Brown, G. F. (1972) Tectonic map of the Arabian Peninsula, *Saudi Arabian Peninsula Map AP-2.* Saudi Arabian Dir. Gen. Miner. Resour.

Coleman, R. G. (1977) *Ophiolites. Ancient Oceanic Lithosphere?* Springer-Verlag, Berlin, 229 p.

Dziewonski, A. M. and **Hales, A. L.** (1972) Numerical Analysis of dispersed seismic waves. In: B. Alder, S. Frenbach and M. Rotenberg **(Ed)**, *Methods in Computational Physics.* Academic Press, New York, NY, 39-85.

Ghalib, H. A. A. (1992) *Seismic velocity structure and attenuation of the Arabian Plate Thesis,* Saint Louis University, Saint Louis, Missouri, USA, 350 p.

Herrmann, R. B. (1987) *Computer Programs in Seismology,* I-VII. Saint Louis University, Saint Louis, Missouri, USA.

Iyer, H. M. and **Hirahara, K.** (1993) *Seismic Tomography - Theory and Practice,* Chapman and Hall, London.

Levshin, A. L., Yanovskaya, T. B., Lander, A. V., Bukchin, B. G., Barmin, M. P., Ratnikova, L. I. and **Its, E. N.** (1989) *Seismic surface waves in laterally inhomogeneous Earth,* V. I. Keilis-Borok **(Ed)** Kluwer Publ., Dordrecht, Holland.

Maamoun, M. (1976) *La seismicite du Moyenet du Proche-Orient dans le cadre de la seismotectonique mondiale. These, Doc. Sci.,* Univ. Louis Pasteur, Strasbourg.

McNamara, D. E., Hazler, S. E. and **Walter, W. R.** (1997) Velocity structures across northern Africa, southern Europe, the Middle East and the Arabian Peninsula from surface waves dispersion , *EOS,* **78:** F499.

Mellors, R. J., Vernon, F. and **Al-Amri, A. M**. (1997) Characterization of Regional Waveform propagation in the Saudi Arabian Peninsula by Waveform stacking (Abstract). *American Geophyiscal Union Fall Meeting* **78**(46): F428.

Mokhtar, T. A., Ammon, C. J., Ghalib, H. A. A. and **Herrmann, R. B.** (1997) Lithospheric structures beneath Arabia (Abstract). *American Geophysical Union Fall Meeting* **78**(46): F499.

Mokhtar, T. A. and **Al-Saeed, M. M.** (1994) Shear wave velocity structures of the Arabian Peninsula, *Tectonophysics,* **230:** 105-125.

Mokhtar, T. A. (1995) Phase velocity of the Arabian Platform and the surface waves attenuation characteristics by wave from modeling, Jour. King Abdulaziz Univ., *Earth Sci.***, 8:** 23-45.

Mooney, W. D., Gettings, M. E., Blank, H. R. and **Healy, J. H.** (1985) Saudi Arabian seismic deep-refraction profile: a travel time interpretation of crustal and upper mantle structure. *Tectonophysics,* **111:** 173-246.

Nolet, G. (1987) *Seismic Tomography*, D. Reidel Publishing Company, Dordrecht, Holland.

Paige, C. C., and **Saunders, M. A.** (1982) LSQR: An algorithm for sparse linear equations and sparse least squares, *ACM Trans. Math. Softw.,* **8:** 43-71.

Powers, R. W., Ramirez, L. F., Redmond, C. P. and **Elberg, E. L.** (1966) Geology of the Arabian Peninsula-sedimentary geology of Saudi Arabia. *U. S. Geol. Surv. Prof. Pap. 560-D,* 147 p.

Ritzwoller, M. H. and **Levshin, A. L.** (1998) Eurasian surface wave tomography: Group velocities, *J. Geophys. Res.,* **103:** 4839-4878.

Ritzwoller, M, H., and Levshin, A. L., Ratnikova, L. I. and **Egorkin, A. A.** (1998) Intermediate period group velocity maps across central Asia, western China, and parts of the Middle East, (in press).

Rodgers, A., Walter, W., Zhang, Y. S., Mellors, R. J. and **Al-Amri, A. M.** (1997) Lithospheric structure of the Middle East from complete waveform modeling (Abstract). *American Geophysical Union Fall Meeting* **78**(46): F495.

Roobol, M. J. and **Al-Rehaili, M.** (1997) Geohazards along the Makkah-Madinah-Nafud (MMN) volcanic line, Saudi Arabian Deputy Ministry for Mineral Resources Technical Report *DMMR-TR-97-1,* 125-140.

Sandvol, E., Seber, D., Barazangi, M., Vernon, F., Mellors, R. and **Al-Amri. A.** (1998) Lithospheric velocity discontinuities beneath the Arabian Shield, *Geophys. Res. Lett.*, **25:** 2873-2876.

Schmidt, D. L., Hadley, D. G. and **Stoeser, D. B.** (1979) Late Proterozoic crustal history of the Arabian Shield, southern Najd province, Kingdom of Saudi Arabia, evolution and mineralization of the Arabian-Nubian shield. *I. A. G. Bull.,* **3**(2): 41-58.

Stoeser, D. B. and **Camp, V. E.** (1985).Pan-African microplate accretion of the Arabian Shield. *Bull Geol. Soc. Am.,* **96:** 817-826.

Vernon, F. and **Berger, J.** (1997) Broadband seismic characterization of the Arabian Shield, *Interim scientific and technical report,* 17 p.

Woodhouse, J. H. and **Dziewonski, A. M.** (1984) Mapping the upper mantle: Three-dimensional Modeling of the earth structure by inversion of seismic waveforms, *J. Geophys. Res.***, 89:** 5953-5986.

Wu, F. T. and **Levshin, A.** (1994) Surface-wave group velocity tomography of East Asia, *Physics of the Earth and Planetary Interiors,* **84:** 59-77.

التركيب الطموغرافي للغلاف الصخري تحت الجزيرة العربية باستخدام سرعة المجموعة للموجات السطحية

طلال مختار* ، تشارلز آمون ، روبرت هيرمان** و حافظ غالب*****

* *قسم الجيوفيزياء ، كلية علوم الأرض ، جامعة الملك عبد العزيز*
جـــدة – المملكة العربية السعودية
** *قسم علوم الأرض والجو ، جامعة سانت لويس*
سانت لويس ، ميـــزوري – الولايات المتحدة الأمريكية
*** *سايك ، ساوث باتريك درايف ، سويت ، ساتلايت بيتش*
فـــلوريدا – الولايات المتحدة الامريكية

المستخلص . تم احتساب توزيع سرعة المجموعة الزلزالية في الأبعاد الثلاثة تحت الصفيحة العربية باستخدام الموجات السطحية رايلي ولف . كما تم بصورة متوازنة تغطية مسارات الموجات السيزمية المنبثقة من الهزات الأرضية على حدود الصفائح في البحر الميت وخليج العقبة وخليج عدن وغرب إيران وتركيا وفوالق أخدود البحر الميت . وتم قياس تغيير سرعة المجموعة لكل من موجات رايلي وموجات لف بتطبيق تقنية تحليل المرشح المتعدد ثم تطبيق تقنية الطموغرافيا (الرسم الطبقي) الانعكاسي باستخدام هذه المشاهدات وذلك لحساب التغيرات الجانبية في سرعة المجموعة للزمن الدوري من ٥ إلى ٦٠ ثانية . وقد وجد أن نتائج كل من موجات رايلي وموجات لف متطابقة وتبين أن متوسط سرعة المجموعة تزداد من ٢,٣٨ كم/ ث و ٢,٤٤ كم/ ث عند ٥–٧ ثانية إلى ٣,٧٤ كم/ ث و ٣,٩٨ كم/ ث عند ٥٦–٦٠ ثانية لكل من موجات رايلي ولف على الترتيب .

إن نتائج الرسم الطبقي قد حددت أيضًا بدقة التغير الإقليمي من الرتبة الأولى في عدم التجانس في التركيب ، بالإضافة إلى تحديد الحد الفاصل بدقة للانتقال بين الوحدتين التكوينيتين في المنطقة وهما الدرع العربي (أسرع من المتوسط) والرصيف القاري العربي (أبطأ من المتوسط) .